The Analysis of Medium-Sized Arrays of Complex Elements Using a Combination of FDTD and Reaction Matching

Chris J. Railton, *Member, IEEE,* and Geoffrey S. Hilton

***Abstract*— The analysis of medium-sized arrays of complex antenna elements by means of a full-wave technique often requires impractical amounts of computer power. Nevertheless, it is essential that all the mutual couplings between elements are taken into account. In this contribution, a technique is presented in which the individual element is characterized using the FDTD method and, using the information this provides, the behavior of the complete array is predicted using a method based on reaction matching. Results using this method are compared to measurement and to results obtained using a complete full-wave analysis for three-and five-element arrays of printed dipoles. The error introduced by the approximation is shown to be small in most cases. For arrays of between 10 and 50 elements, savings in computer time of several orders of magnitude can be achieved and, in addition, changes in array geometry do not always necessitate all the results being recalculated.**

***Index Terms*—Antenna arrays, FDTD, printed antennas.**

I. Introduction

THE prediction of the far-field radiation patterns and return losses of finite antenna arrays comprising elements, such as printed dipoles of the type described in [1], is doubly problematic. First, even the analysis of a single element is difficult, and second, calculation of the interaction between array elements, which are placed in close proximity, increases the scale of the problem enormously. This is true regardless of whether techniques such as FDTD [2] or the method of moments [3] is used. For FDTD, although the computational effort is only linearly dependent on the size of the computational space, the discretization of the total space occupied by the array is necessary. For the method of moments the effort is proportional to some power of the number of unknowns. For medium-sized arrays of between five and 50 closely spaced complicated elements where infinite array approximations are inadequate but where mutual impedance effects cannot be ignored, the situation using either technique rapidly becomes impracticable. In previous work [4], a general method for drastically reducing the amount of computer resources required for this type of problem was developed. This was shown to give excellent results for the case of an array of wire dipoles but when the antenna elements are more complicated the results were somewhat disappointing. In this contribution, the reasons for the variation in performance between the two different element types is examined and a way of extending the methodology in order to improve the results is presented. This novel method is shown to yield accurate results for arrays of printed dipoles [1] while still using just a medium power workstation, namely the HP9000/730. The FDTD program used was developed at the University of Bristol and for the analysis of an individual array element a nonuniform mesh of size $80 \times 32 \times 72$ cells was used and 17 000 time steps of 0.261 ps were taken.

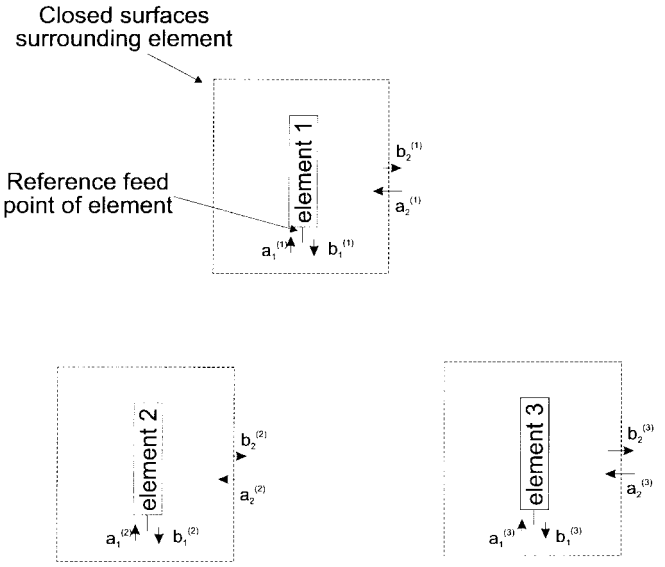

Fig. 1. The basic problem to be solved.

Results obtained for arrays consisting of three and five printed dipole elements are presented and compared both to measurements and also to results obtained using a full FDTD analysis. In each case, the error is shown to be small in most cases.

II. Theory

An example of the general problem to be solved is shown in Fig. 1, where three elements of an array are shown. The actual element which will be used as an example in this paper is shown in Fig. 2. Around each element a fictitious extrapolation surface is drawn, shown as a dotted line, on which the scattered

Manuscript received July 2, 1997; revised December 8, 1997. This work was supported by the Defence Evaluation and Research Agency, U.K.

The authors are with the Centre for Communications Research, Faculty of Engineering, University of Bristol, Bristol BS8 1TR, U.K.

Publisher Item Identifier S 0018-926X(99)04777-8.

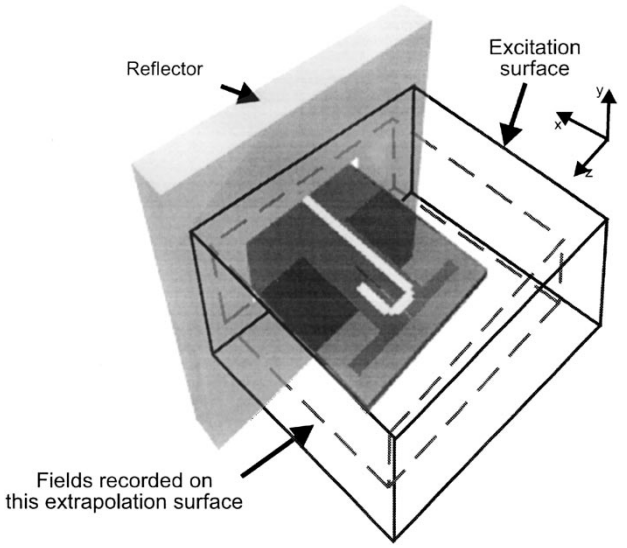

Fig. 2. The array element showing the excitation and reference surfaces.

field patterns of that element in isolation are calculated. In addition another surrounding *excitation* surface (shown as a solid line) is defined, at which incident field distributions may be introduced. Each element with its surrounding surfaces is represented as a two-port network. Because the response of the element to an incident signal at the feedline is different from its response to an incident field from a distant source, each element is characterized for both situations.

In order to get the information which is required, several different test signals are applied to the isolated element. The choice of these test signals is discussed below. In each case the resulting scattered field at the surrounding extrapolation surface and the strength of the signal emanating from the feedline is calculated. The procedure may be summarized as follows:

Test 1—Response to a Signal at the Feedline: Apply a signal having a voltage of u^t to the feed line. Calculate the reflected voltage v^t, and the distribution of the tangential field components on the surrounding extrapolation surface, $\{E^t, H^t\}$. It can be seen that v^t/u^t is the reflection coefficient of the isolated element. The mode of the antenna which is excited by this test is referred to as the *transmit mode*.

Tests 2—Response to Incident Test Fields: Apply a number of incident test fields having distributions $\{E^{ip}, H^{ip}\}$ at the surrounding excitation surface. In each case calculate the strength of the signal emanating from the feed line v^p and the distribution of the scattered field at the surrounding extrapolation surface, $\{E^{op}, H^{op}\}$. It is noted that this requires P separate FDTD runs, where P is the number of test fields used.

A. The Basic Reaction Integral Approach

In the basic reaction integral approach described briefly in [4], there is only a single incident test field in Test 2. For the complete array, the total incident field on the surrounding surface of the ith element is designated $\{E^{\text{inc}}, H^{\text{inc}}\}$. This can be expressed as follows:

$$E_i^{\text{inc}} = \sum_{j \neq i} E_{ij}^r + \frac{a_1^{(j)}}{u_0} E_{ij}^t \tag{1}$$

$$H_i^{\text{inc}} = \sum_{j \neq i} H_{ij}^r + \frac{a_1^{(i)}}{u^0} H_{ij}^t \tag{2}$$

where a_1^i is the excitation applied to the feedline of element i, (E_{ij}^r, H_{ij}^r) and (H_{ij}^t, E_{ij}^t) are the fields incident on the surrounding surface of element i due to a scattered field $\{E_j^r, H_j^r\}$ and $\{E^t, H^t\}$, respectively, on the surrounding surface of element j. These are calculated using the method described in [5]. The fields $\{E_j^r, H_j^r\}$ are the total scattered fields at the surrounding surface of element j, and the fields $\{E_j^t, H_j^t\}$ are the fields on the surrounding surface of element j caused by unit excitation of the feedline of element j.

The scattered field from element i can be approximated as being proportional to the field $\{E^o, H^o\}$ obtained from Test 2, in the following manner:

$$E_i^r \simeq c_i E^o \quad H_i^r \simeq c_i H^0 \tag{3}$$

where

$$c_i = \frac{\langle E_i^{\text{inc}}, H^o \rangle - \langle E^o, H_i^{\text{inc}} \rangle}{\langle E^i, H^o \rangle - \langle E^o, H^i \rangle} \tag{4}$$

with the inner product defined as

$$\langle \boldsymbol{a}, \boldsymbol{b} \rangle = \int_{\text{surface}} \hat{n} \cdot (\boldsymbol{a} \times \boldsymbol{b})\, dS \tag{5}$$

and n is the unit vector normal to the surface.

The accuracy of this approximation depends upon how closely the total incident field distribution is represented by the test field $\{E^i, H^i\}$ and on the dependence of the scattered field from the element on the form of the incident field. Clearly, if the actual incident field is the same as the test field, then (4) will be exact. In practice, choosing a test field which is a good approximation to the actual incident field will result in good accuracy.

Taking the inner products of (1) and (2) with H^o and E^o, respectively, subtracting and substituting from (4) yields

$$c_i = \sum_{i \neq j} c_j \frac{\langle E^o, H_{ij}^o \rangle - \langle E_{ij}^o, H^o \rangle}{\langle E^o, H^i \rangle - \langle E^i, H^o \rangle} + \frac{a_1^{(j)}}{u_t} \langle \frac{\langle E^o, H_{ij}^t \rangle - \langle E_{ij}^t, H^o \rangle}{\langle E^i, H^o \rangle} \tag{6}$$

or rearranging

$$c_i(\langle E^o, H^i \rangle - \langle E^i, H^o \rangle) + \frac{a_1^{(j)}}{u^t}(\langle E^o, H_{ij}^t \rangle - \langle E_{ij}^t, H^o \rangle). \tag{7}$$

This can be expressed in matrix form as follows:

$$\boldsymbol{c} = \boldsymbol{P}^{-1} \boldsymbol{Q} \frac{\boldsymbol{a}}{u^t} \tag{8}$$

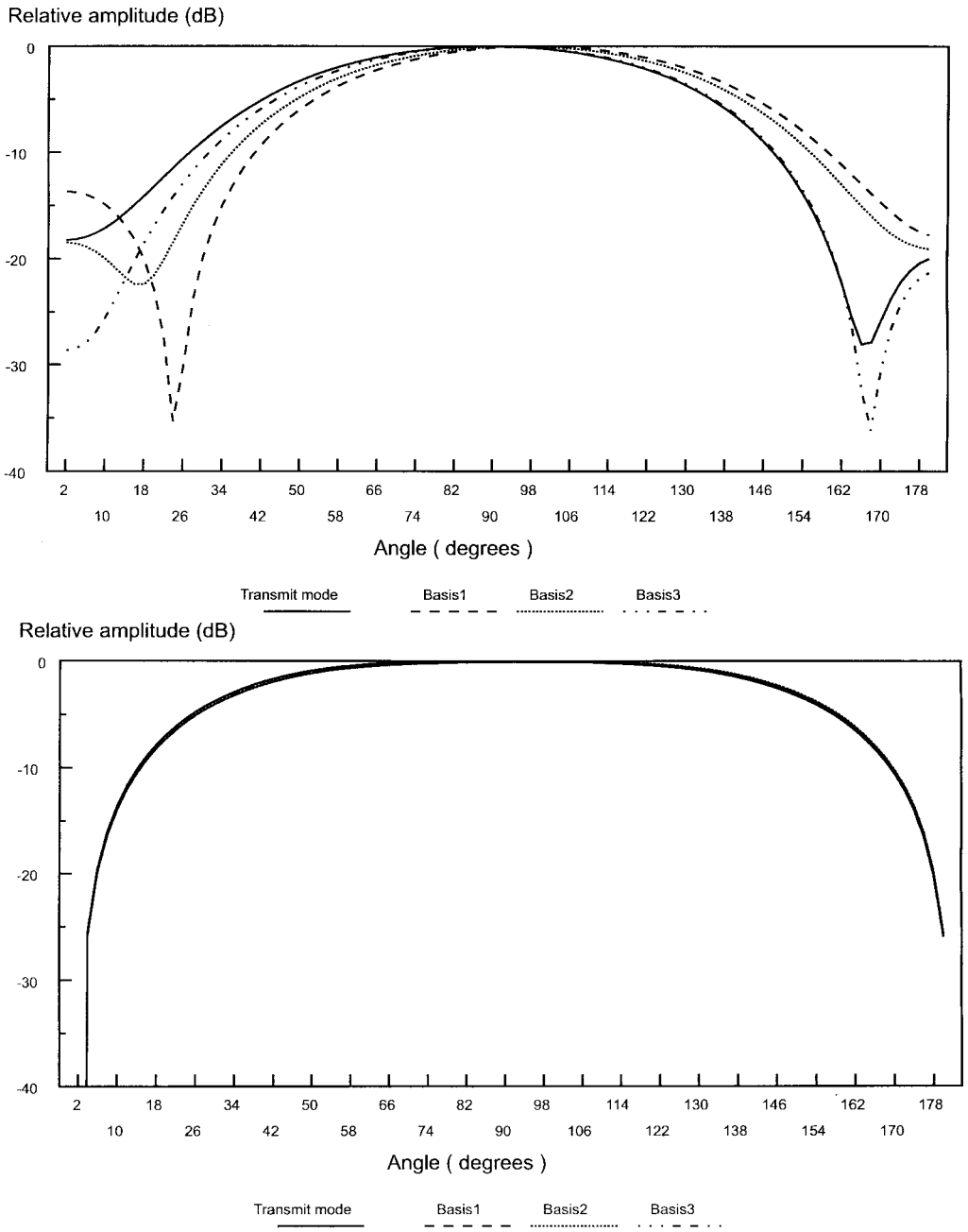

Fig. 3. The scattered field pattern in response to different incident fields.

where

$$\boldsymbol{P}_{ij} = -\langle E^o, H^o_{ij}\rangle + \langle E^o_{ij}, H^o\rangle \qquad i \neq j \tag{9}$$

$$\boldsymbol{P}_{ij} = \langle E^o, H^i\rangle - \langle E^i, H^o\rangle \qquad i = j \tag{10}$$

$$\boldsymbol{Q}_{ij} = \langle E^o, H^t_{ij}\rangle - \langle E^t_{ij}, E^o\rangle \qquad i \neq j \tag{11}$$

$$\boldsymbol{Q}_{ij} = 0 \qquad i = j. \tag{12}$$

From the result of Test 2 we can deduce that if the feedline of element i is not excited

$$\frac{b_1^{(i)}}{v} = c_i \tag{13}$$

where b_1^i is the strength of the signal emanating from the feedline of element i of the array.

Hence the array S matrix is given by

$$\boldsymbol{S} = \boldsymbol{P}^{-1}\boldsymbol{Q}\frac{v}{u^t} + \boldsymbol{I}\frac{v^t}{u^t} \tag{14}$$

where $\boldsymbol{I}$ is the unit matrix.

It is noted that in all cases the matrix $\boldsymbol{P}$ was well conditioned and no problems were encountered in inverting it.

While this method gave excellent results for the case of the array of wire dipoles [4], when the analysis of an array of printed dipoles was attempted, the accuracy achieved was not sufficient. The reasons for this are discussed in the following section.

B. Limitations and Extension of the Basic Reaction Integral Method

In the basic method, only one incident test field is used for Test 2. The approximation is then made that the distribution of the scattered field resulting from the actual incident field will be the same as the distribution of the scattered field which results from the incident test field. This corresponds to the assumption that the induced current distribution on the antenna is independent of the form of the incident signal. For the wire dipole treated in [4] this is indeed very nearly the case. However, for the more complicated case of the printed dipoles, it has been found that the direction from which the incident field arrives can make a considerable difference to the form of the scattered field. This behavior is illustrated in Fig. 3 which shows the scattered fields in the E plane and the H plane of the element resulting from incident fields impinging from three different directions corresponding to the positions of three different neighbors in the array shown in Fig. 4. It can be seen that, whereas in the H plane, the scattered field is indeed virtually independent of the direction of the incident field, this is definitely not the case for the E plane. In particular, it can be seen that the characteristic null in the radiation pattern which exists at around 70° from boresight when the feedline is excited, changes position depending on the direction of the incident excitation.

In view of this behavior, it was considered necessary to extend the basic method in order to allow the inclusion of several test fields so that the effects of the direction of arrival of the incident fields could be accounted for. Since the basic method does not directly lend itself to multiple test functions, a different way forward was sought. Rather than using all the available test fields at once, each test field is used individually to provide separate estimates of the array S matrix. Thus, if the six test fields indicated in Fig. 4 were used, there would be six estimates of the S matrix of the complete array, each estimate corresponding to a chosen test field, given by

$$\boldsymbol{S}^{(p)} = (\boldsymbol{P}^{(p)})^{-1}\boldsymbol{Q}^{(p)}\frac{v^p}{u^t} + \boldsymbol{I}\frac{v^t}{t^t} \tag{15}$$

where $\boldsymbol{I}$ is the unit matrix. The second term on the right-hand side of (15) represents the reflection of the signal incident at the feedlines of an element in isolation, while the first term represents the additional reflected signal due to scattering by the other elements in the array.

C. Calculation of the Array $\boldsymbol{S}$ Matrix

As has previously been discussed in Section II-B, the incident field at an array element will depend on which of the other elements are being excited. If the field distribution at the excitation surface of element 1 resulting from excitation of element 2, labeled 1 in Fig. 4, was used as a test field, then the actual incident field at element 1 would be similar to the test field as long as only element 2 was excited. The difference between the actual field and the test field under that condition is caused only by multiple scattering from neighboring elements and will, therefore, normally be small. The corresponding value of S_{12} calculated using this test function would be expected, therefore, to be accurate but the other S parameters calculated this way are likely to exhibit greater error. Similarly, if the field distribution labeled 2 in Fig. 4 was used as the test function, then an accurate result would be expected for S_{13}. In order to calculate accurate results for all six off-diagonal S parameters, Test 2 may be carried out for each of the six test fields shown in Fig. 4 then each S parameter would be selected from the test is considered to provide the most accurate result. This is expressed as follows:

$$\boldsymbol{S} = \begin{pmatrix} S_{11}^{(1)} & S_{12}^{(1)} & S_{13}^{(2)} \\ S_{21}^{(3)} & S_{22}^{(2)} & S_{23}^{(6)} \\ S_{31}^{(4)} & S_{32}^{(5)} & S_{33}^{(3)} \end{pmatrix} \tag{16}$$

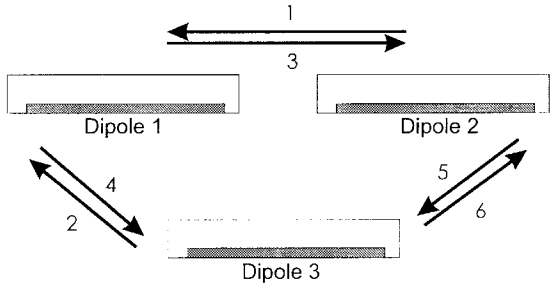

Fig. 4. The six possible "nearest neighbor" test fields.

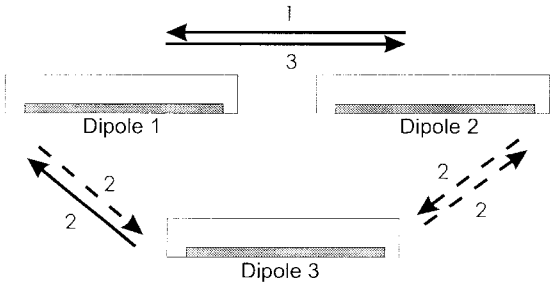

Fig. 5. Test fields used for each pair of dipoles. Solid lines show that test fields have been derived using the pair.

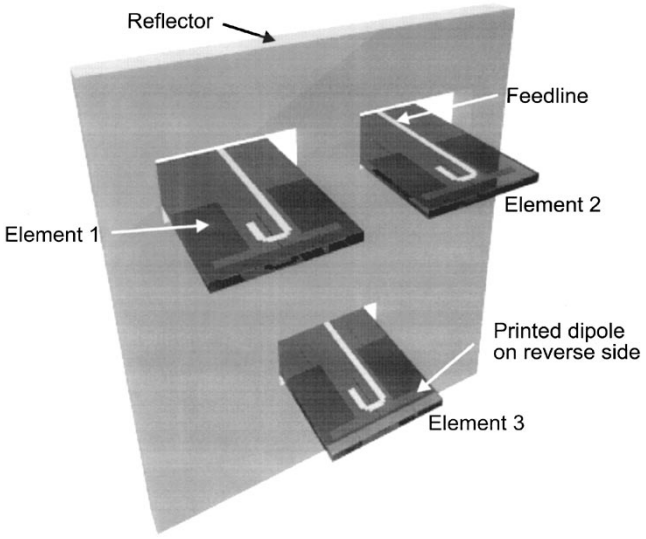

Fig. 6. The arrangement of the three element array.

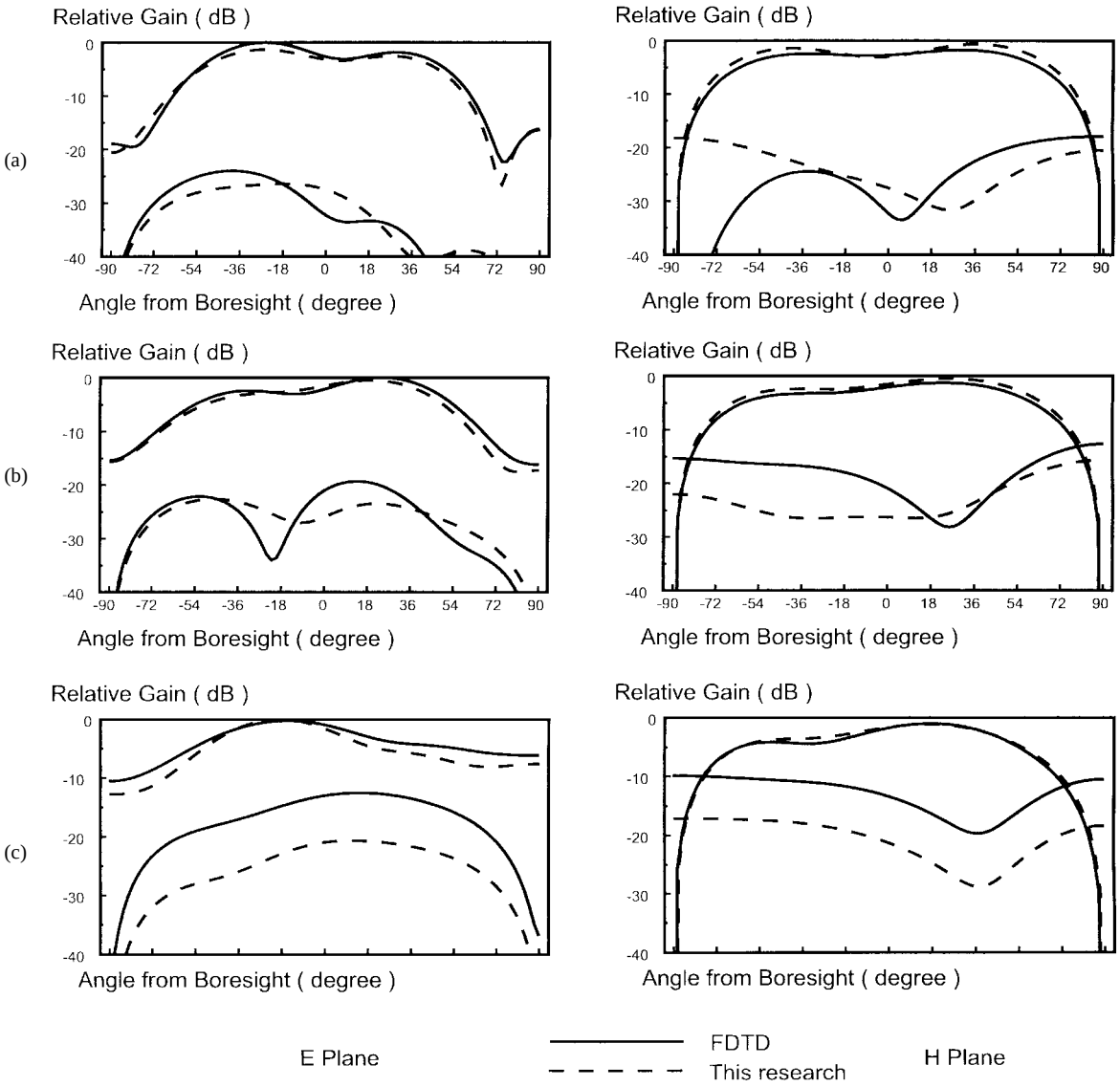

Fig. 7. Embedded radiation patterns for the three-element array. (a) 9 GHz, (b) 10 GHz, and (c) 11 GHz. Element 1 excited.

which shows that S_{12} is calculated using test field 1, S_{13} is calculated using test field 2 and so on.

A selection matrix D is defined for an array which specifies which estimate to use for each component of the array S matrix

$$S_{i,j} = S_{i,j}^{(D_{i,j})}. \tag{17}$$

In this case D would be

$$\boldsymbol{D} = \begin{pmatrix} X & 1 & 2 \\ 2 & X & 6 \\ 4 & 5 & X \end{pmatrix} \tag{18}$$

i.e., each element of the S matrix would be calculated using the test function which is the incident field on the target element caused by feedline excitation on the source element. The X's in the diagonal position indicate that no particular test function would be expected to yield a lower error than any other so, in this case, any of the test functions may be used.

In order to reduce computational requirements, it is advantageous to use fewer than six test functions. In that case each S parameter would be taken from the test in which the actual field would be closest to the test field. For instance, consider the case where three test functions are used as shown in Fig. 5 which are derived as follows:

Function 1	source element 2	target element 1
Function 2	source element 3	target element 1
Function 3	source element 1	target element 2.

Any of these functions may be used to approximate the field arriving at a specified element resulting from excitation at a different specified element. In Fig. 5, one possible choice is shown. Here the pairs of elements, which have not been used to provide test functions, are assigned test functions that are considered to be the best approximation. The solid lines show the pairs of elements from which the test functions have been derived; the dashed lines in Fig. 5 show those pairs of elements for which the closest available test function has been used instead. Clearly, other choices are possible. The matrix

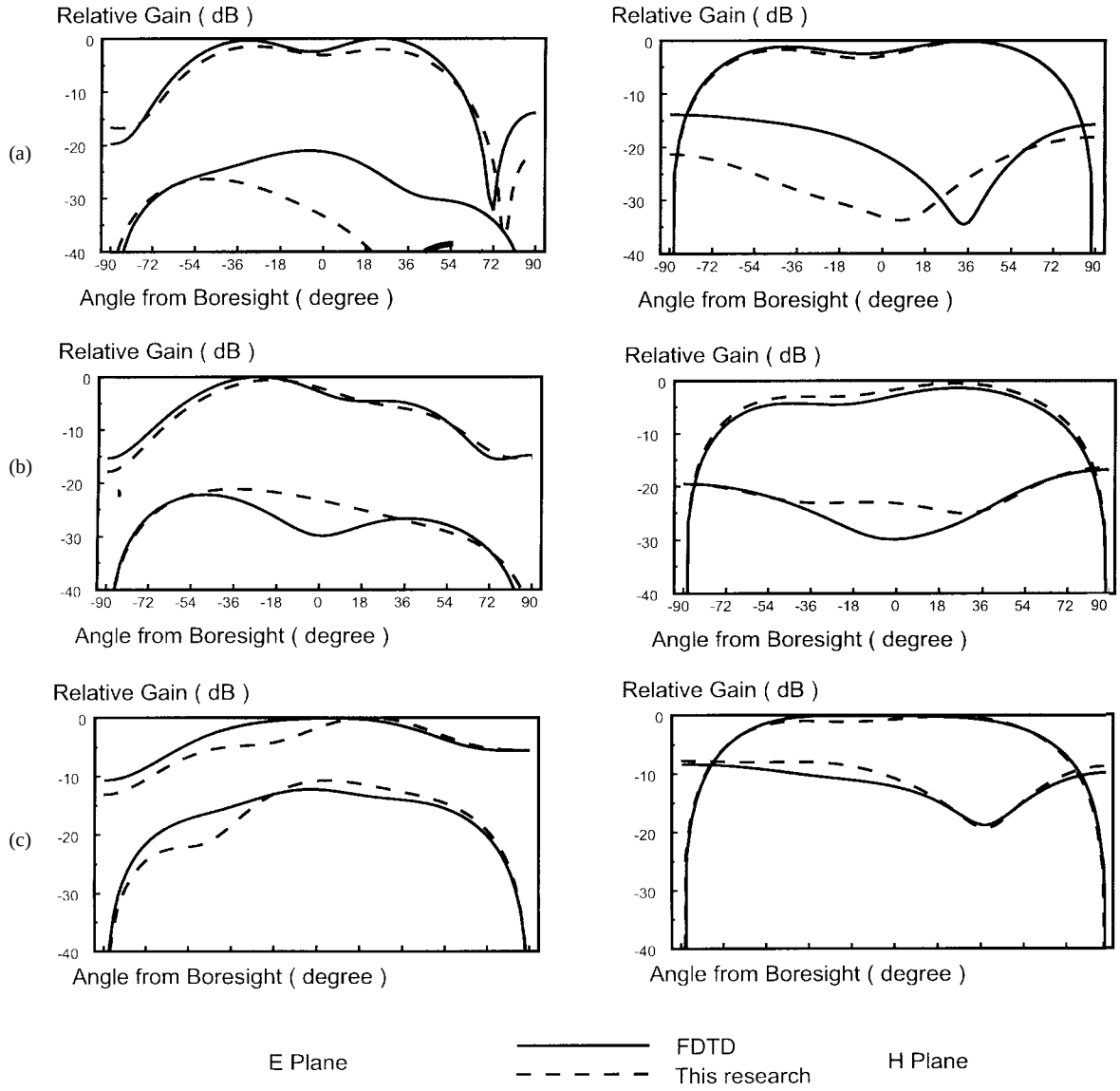

Fig. 8. Embedded radiation patterns for the three-element array. (a) 9 GHz, (b) 10 GHz, and (c) 11GHz. Element 2 excited.

D in this case is given by

$$\boldsymbol{D} = \begin{pmatrix} X & 1 & 2 \\ 3 & X & 2 \\ 2 & 2 & X \end{pmatrix}. \tag{19}$$

D. Calculation of the Far Field Radiation Patterns

From the results of Test 2, the far-field patterns corresponding to each of the scattered fields, $\{E^{op}, H^{op}\}$ are calculated and are designated as $\{E^{fp}, H^{fp}\}$. Similarly the far-field pattern corresponding to excitation of the feedline is designated $\{E^{ft}, H^{ft}\}$. The total far-field pattern is then given by

$$E^F = \sum_j \frac{\boldsymbol{a}_j}{u^{(t)}} \sum_i \boldsymbol{C}_{i,j}^{D_{i,j}} E^{fD_{i,j}}. \tag{20}$$

Hence, once the matrix C and the far-field patterns corresponding to each test function has been calculated, the far-field pattern corresponding to any excitation vector can be speedily determined.

E. The Far-Field Radiation Patterns of the Three-Element Array

As an initial trial of the method, the three-element array illustrated in Fig. 6 was addressed. Results at frequencies of 9, 10, and 11 GHz are shown in Figs. 7 and 8 where a comparison is made between a full FDTD analysis (solid lines) and the extended reaction integral method (dashed lines). It can be seen that for the copolar patterns the agreement is generally within ± 1 dB, the discrepancy is somewhat larger for the cross-polar results but the general shape and magnitude of the curves are correctly predicted. The full FDTD analysis required approximately three times the computer run-time as the new method. All calculations in this section assume an infinite ground plane.

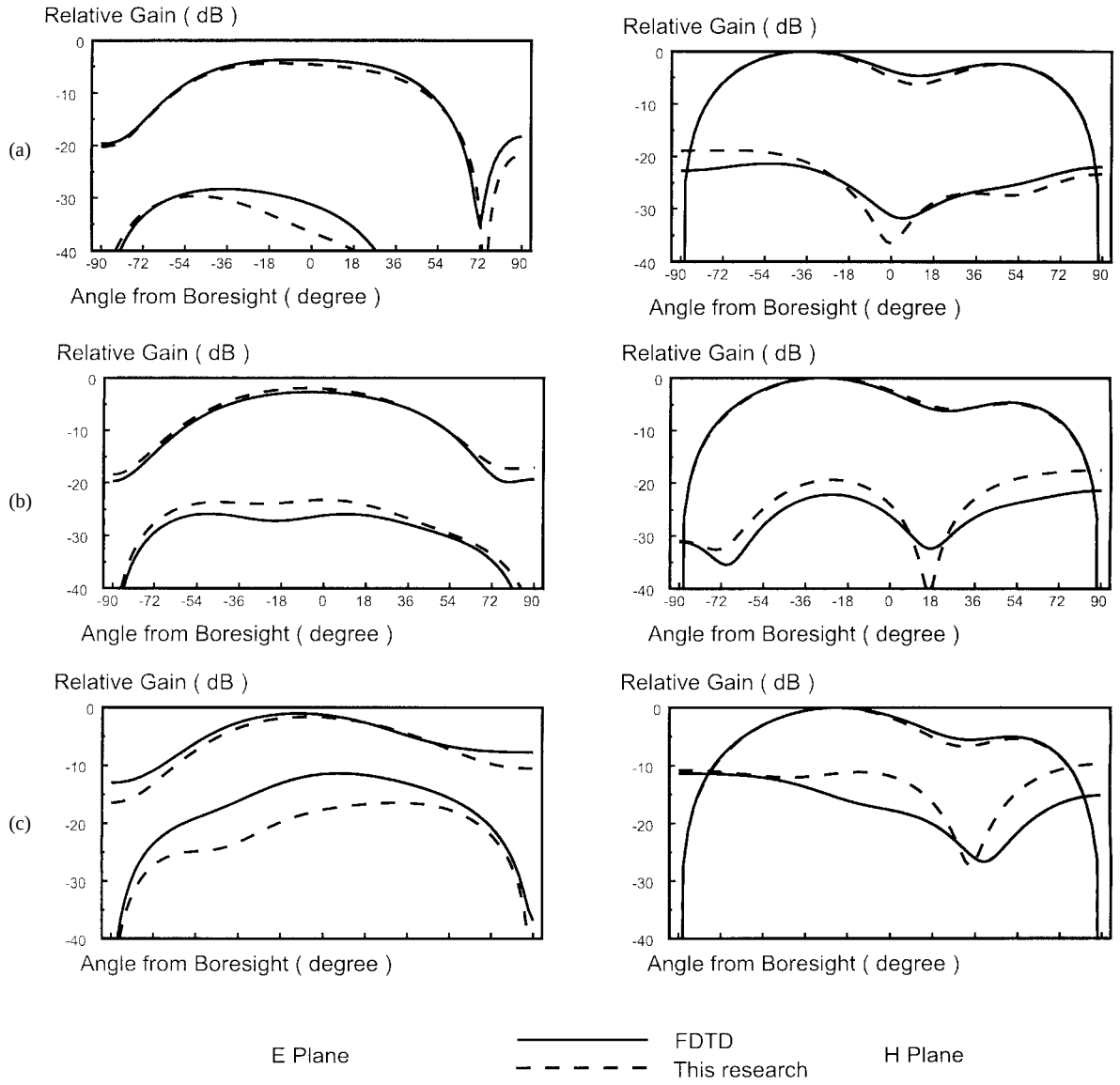

Fig. 9. Embedded radiation patterns for the three-element array. (a) 9 GHz, (b) 10 GHz, and (c) 11 GHz. Element 3 excited.

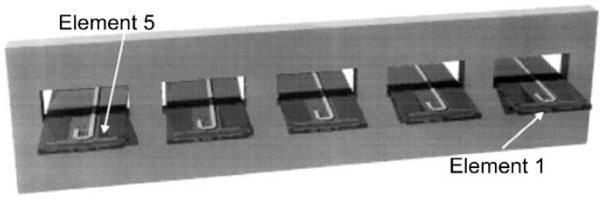

Fig. 10. The layout of the five-element array.

F. The Far Field Radiation Patterns of the Five-Element Array

The radiation patterns of the five-element linear array shown in Fig. 10 was also analyzed and measured. The spacing between elements was again 18 mm. Results for the embedded radiation patterns for each element in the array are given in Figs. 11–15. The solid lines are measured results and the dashed lines are those predicted using the reaction integral technique. In addition, a full FDTD run was performed for the case when the center element (element 3) is excited. This is shown as the dotted line in Fig. 13. For all the calculated results, the ground plane was assumed to be infinite in extent while for the measurements, a ground plane of diameter 34 cm was used. This was considered large enough so as to have negligible effect on the overall radiation pattern.

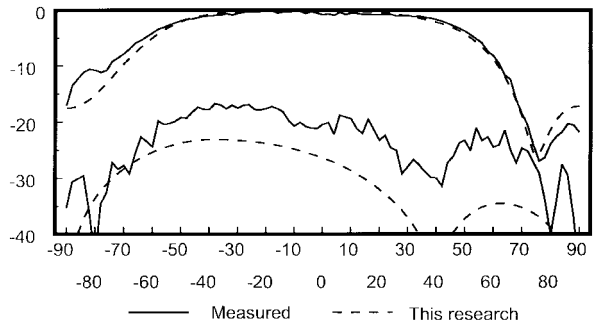

Fig. 11. *E*-plane radiation pattern of the five-element array at 9.3 GHz. Element 1 excited.

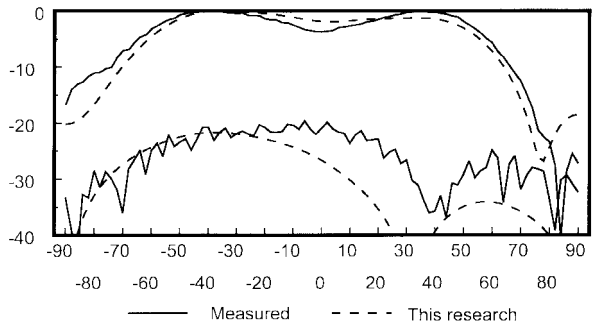

Fig. 12. E-plane radiation pattern of the five-element array at 9.3 GHz. Element 2 excited.

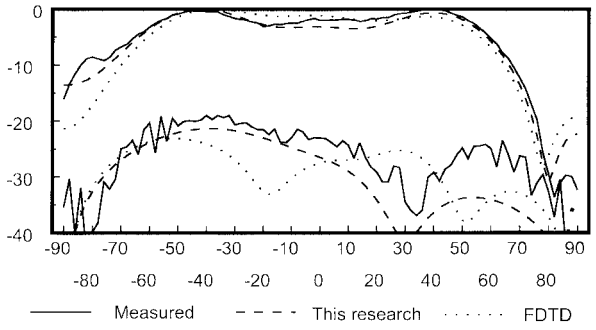

Fig. 13. E-plane radiation pattern of the five-element array at 9.3 GHz. Element 3 excited.

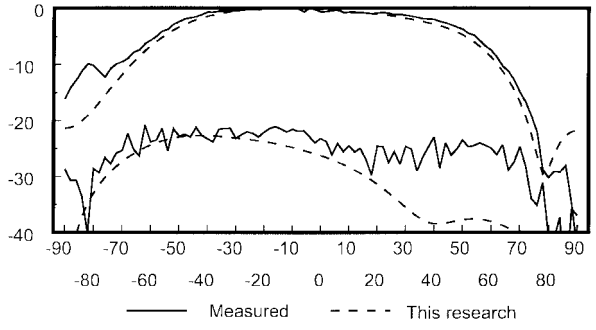

Fig. 14. E-plane radiation pattern of the five-element array at 9.3 GHz. Element 4 excited.

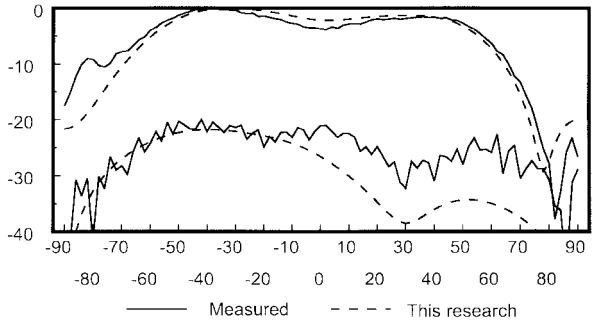

Fig. 15. E-plane radiation pattern of the five-element array at 9.3 GHz. Element 5 excited.

Again, it can be seen that in almost all cases the agreement for the copolar radiation pattern is better than ± 1 dB and that the predictions for the cross-polar patterns show the same features and with reasonable agreement for the magnitudes. In this case a full FDTD run is estimated to have taken nine times as long as the new method. For this reason an FDTD run was only performed for one excitation vector.

III. Conclusions

In this paper, a novel technique for the analysis of medium sized antenna arrays has been demonstrated to provide accurate results even when the individual elements are closely spaced and have a complicated geometry. Improvements in computer time of an order of magnitude have been achieved for the case of a five-element array. It is estimated that this improvement would be about two orders of magnitude for arrays of between 20–30 elements. In addition, the memory requirement is reduced by a factor approximately equal to the number of elements in the array.

References

[1] G. S. Hilton and C. J. Railton, "Finite-difference time-domain analysis of a printed dipole antenna," in *Inst. Elect. Eng. 9th Int. Conf. Antennas Propagation*. Eindhoven, The Netherlands, vol. 1, Apr. 1995, pp. 72–75.

[2] K. S. Kunz and R. J. Leubbers *The Finite Difference Time Domain for Electromagnetics*. Boca Raton, FL: CRC, 1993.

[3] R. F. Harrington *Field Computation by Moment Methods*. Piscataway, NJ: IEEE Press, 1993.

[4] C. J. Railton, S. A. Meade, and G. S. Hilton "New methodology for the analysis of finite arrays of complex antenna elements," *Electron. Lett.*, vol. 32, no. 9, pp. 784–785, Apr. 1996.

[5] I. J. Craddock and C. J. Railton, "Application of the FDTD method and a full time-domain near-field transform to the problem of radiation from a PCB," *Electron. Lett.*, vol. 29, no. 23, pp. 2017–2018, Nov. 1993.

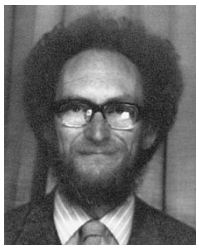

Chris J. Railton (M'88) received the B.Sc. degree in physics with electronics from the University of London, U.K., in 1974 and the Ph.D. degree in electronic engineering from the University of Bath, U.K., in 1988.

From 1974 to 1984, he worked in the scientific civil service on a number of research and development projects in the areas of communications, signal processing and EMC. Between 1984 and 1987 he worked at the University of Bath on the mathematical modeling of boxed microstrip circuits. He currently works in the Centre for Communications Research at the University of Bristol where he leads the Computational Electromagnetics Group, which is involved in the development of new algorithms and their application to MMIC's, planar antennas, optical waveguides, microwave and RF heating, and EMC and high-speed logic.

Geoffrey S. Hilton received the B.Sc. degree from the University of Leeds, U.K., in 1984 and the Ph.D. degree from the Department of Electrical and Electronic Engineering at the University of Bristol, U.K., in 1992.

From 1984 to 1986, he worked as a Design Engineer at GEC-Marconi, before commencing research on Microwave Antennas, first as a postgraduate and later as a member of research staff, at Bristol University. The work included design and analysis of printed antenna elements and arrays, and involved the development of FDTD models for these structures and comparison with measured data. In 1993 he joined the academic staff, lecturing in microwave antennas and satellite communications. Current research interests include radiation pattern synthesis and array modeling, synthetic focusing ground penetrating radar, and the design of electrically small antennas and active antennas for mobile communications applications.